EUROPEAN ORGANISATION FOR NUCLEAR RESEARCH

CERN-EP/86-33
March 10th, 1986

MAGNETIC BIREFRINGENCE MEASUREMENT IN HYDROGEN AND DEUTERIUM GASES.

F.Scuri[1], G.Stefanini[1], E.Zavattini[1],
S.Carusotto[2], E.Iacopini[3], E.Polacco[2]

Geneva, March 7, 1986

Abstract: The first measurement of the magnetic birefringence (Cotton-Mouton effect) in molecular hydrogen and deuterium has been performed. The Cotton-Mouton constant of H_2 and D_2 has been measured at room temperature, atmospheric pressure, and for $\lambda = 514.5$ nm. Comparison with theoretical calculations shows very good agreement in both cases.

PACS: 33, 42.50

(submitted to Journal of Chemical Physics)

---

1) CERN, Geneva, Switzerland.

2) I.N.F.N. Sez. Pisa and University of Pisa, Italy.

3) I.N.F.N. Sez. Pisa and Scuola Normale Superiore of Pisa, Italy.

1. INTRODUCTION

We present here the first measurements of the magnetic birefringence in H_2 and D_2 gases (Cotton-Mouton effect); the measurements were performed relatively to nitrogen, for which accurate experimental values are available in the literature in the visible region and at different conditions of temperature and pressure [1,2,3].

The Cotton-Mouton constant C_{CM} is defined by

$$\Delta n = n_{\parallel} - n_{\perp} = C_{CM} \lambda B^2 \qquad (1)$$

where $n_{\parallel}$ and $n_{\perp}$ are the refraction indices for light linearly polarized parallel and orthogonal to the direction of the applied magnetic field respectively, and B is the field component normal to the optical path.

Measurements of optical properties like the magnetic birefringence on the diatomic molecules H_2 and D_2 are of particular interest since these properties depend on molecular properties for which "ab initio" calculations exist. Calculations of the Cotton-Mouton effect in gases have been developed by Buckingham and Pople [4] and by Kielich [5]. It can be shown that, in the case of H_2 and D_2, the C_{CM} constant can be related in very good approximation to the molecular anisotropies $\Delta\beta$ and $\Delta\chi$ of the electrical polarizability and magnetic susceptibility, respectively, by the following simple relation:

$$C_{CM} = (2\pi N/15V\lambda K_B T)\cdot(\Delta\beta\cdot\Delta\chi) \qquad (2)$$

where N/V is the gas molar density, K_B is the Boltmann constant, T is the absolute gas temperature. Expression (2) was first derived by Neugebauer in 1939 for diatomic molecules in the frame of an approximate general theory [6].

The available calculated values of $\Delta\beta$ and $\Delta\chi$ in H_2 and D_2 are summarized in table 1 and table 2 [7-9]. In the same tables are shown the values of $\Delta\beta$ and $\Delta\chi$ derived respectively from measurements of the depolarization ratio and of the Zeeman effect in rotational transitions [10-13].

From formula (2) it is clear that a measurement of C_{CM} in H_2 and D_2 is a direct determination of the quantity $(\Delta\beta \cdot \Delta\chi)$ that can be compared with the values of $\Delta\beta$ and $\Delta\chi$ given in the literature [7-13].

The measurement of the magnetic birefringence in H_2 and D_2 gases requires a very accurate technique. For this purpose we have developed a very sensitive ellipsometer which measures the ellipticity ψ gained by a linearly polarized light-beam propagating in a gas immersed in transversal magnetic field. The ellipticity ψ is related to the Cotton-Mouton constant by the following expression

$$\psi = \pi C_{CM} \sin(2\theta) \int (B \times k)^2 \, dx \qquad (3)$$

The integration in (3) is performed along the light path, k is the unit vector describing the light propagation direction, θ is the angle between $(B \times k)^2$ and the light polarization vector.

The main features of the ellipsometer are:

i) two independent time modulation are imposed on the effect to be measured;

a) the transverse magnetic field is modulated by rotating a dipole magnet at fixed frquency f_R = 1.3125 Hz and

b) the magnetic field is switched on-off with a period T = 100 seconds. In this way the birefringence effect appears mainly at the two frequencies $2f_R \pm 1/T$ = 2.625±0.010 Hz: These frequencies are sufficiently high to escape from the high noise level in the light polarization state near zero hertz and are well separated from the second harmonic component of the dipole revolving frequency in order to avoid spurious effects due to mechanical vibrations [3].

ii) The birefringence signal is translated to a lower laser noise frequency region by a Faraday cell which modulates the light polarization vector at the frequency f_F = 418.669 Hz and an heterodyne method is used to measure the signal [3].

With the present apparatus the sensitivity ψ_{sens} for the measurement of the light ellipticity is:

$$\psi_{sens} = 3.5 \times 10^{-8} / \sqrt{Hz} \tag{4}$$

and corresponds to a sensitivity Δn_{min} in the gas birefringence of

$$\Delta n_{min} = \psi_{sens} \lambda/(\pi L) = 2.4\ 10^{-16} \tag{5}$$

for an optical path L = 40 cm and 1 hours of integration time.

A description of the experimental apparatus is given in section 2, while the method and the data-aquisition system are described in section 3. The results are discussed in section 4.

2. EXPERIMENTAL APPARATUS

The experimental set-up is shown in figs. 1 and 2. The optical elements and the magnet are shown in fig. 1. The light source is a CW argon ion laser (Coherent Radiation Mod. CR-2) tuned for λ = 514.5 nm and for a light power output W =100 mW.

The beam intensity is monitored by the photodiode D1 via the beam-splitter BS. The Glan-Thompson polarizer P (Karl Lambrecht Inc.) introduces a well-defined polarization state parallel to the horizontal plane. The beam enters the stainless-steel tube T, 2 cm in diameter and 2 m long, which contains the gas under study at 100 mbar above the atmospheric pressure. The tube is evacuated to 10^{-3} Torr before each gas filling. The entrance and exit windows W1 and W2 of the tube are made of BK7 optical flats, 25 mm in diameter, 9 mm thick, mounted with adjustments to minimize the stress birefringence due to pressure differentials.

The central section of the tube is placed in the 4 cm gap of the H-type, iron yoke, dipole magnet (CERN model NP 300 modified). The dipole produces a field B $\approx$ 5.4 KGauss, sharply confined by field clamps to a region 40 cm long.

The dipole of total weight ≈ 500 Kg revolves at the frequency f_R = 1.3125 Hz and is driven by a high-power stepping-motor with belt-drive demultiplication; the dipole is supported on shock-dampers. Proper care is taken to reduce any undesired modulated birefringence. For this purpose the tube containing the gases is well clamped to the ground and the section inside the dipole gap is mechanically isolated by bellows. The entrance window W1 and the exit window W2 are well clamped to the optical benches and they are coupled to the tube T by high resilience bellows. Furthermore, although the residual stray field over the optical elements is not higher than 10^{-3} Gauss, care was taken to place the optical components inside mu-metal shields.

The d.c. excitation current (115 A) is fed to the dipole coils through slip ring contacts and is monitored via a precision resistor; the current is switched on and off every 50 seconds.

A pulse from the small coil SC, derived by inductive coupling from a small permanent magnet fixed to the rotating dipole yoke, is used to synchronize the data aquisition. The pick-up coil PC on the tube T is used to monitor the modulated field B orthogonal to the beam propagation direction.

The light beam traverses the window W2 and the air Faraday cell FCA1 modulated at the frequency f_{a1} = 2.661 Hz, and is directed to the optical phase-shifter OPS [14]. This device transforms the light ellipticity into a pure rotation of the light polarization vector.

The glass Faraday cell FCG introduces a modulation at the frequency f_F = 418.669 Hz in the polarization state which acts as a carrier for the effect to be measured. The air Faraday cell FCA2, modulated at the frequency f_{a2} = 2.649 Hz, produces a reference rotation of the polarization vector. The characteristics of the Faraday cells are given in ref. [3].

The light beam is directed onto the analyser A oriented for maximum extinction. The extinction factor for the crossed prisms P and A is better than 10^{-8}; however, due to the presence of the various optical elements and of the air, the extinction obtained is 10^{-7}, after proper compensation of any the static ellipticity through the compensator C.

The transmitted beam is focoused on the 2.5 mm diameter PIN photodiode D2 used in photovoltaic mode and connected to a low noise current-to-voltage amplifier with feedback resistor of 400 MΩ.

The electronic layout is shown in fig. 2. The various signals for the Faraday cells FCG, FCA1, and FCA2 togheter with the trigger for the stepping motor are derived from synthetizers (HP 3395A) locked to the 5 MHz rubidium master clock.

The Faraday cells currents are measured on-line by a spectrum analyser (HP 3582A) togheter with the signal from the pick-up coil PC. The magnet current value and the output from the diodes D1 and D2 are measured by an A.D.C. at the beginning and at the end of each subrun of 500 seconds.

The D2 signal is also demodulated by a lock-in amplifier (Brookdeal EG&G) referenced to the same signal of the glass Faraday cell FCG. The

output signal is then demodulated by a second lock-in amplifier referenced at twice the magnet rotation frequency, and its output is measured every 10 seconds and stored on the microcomputer. The Fourier transform of the stored data is calculated and displayed at the end of each run.

3. METHOD AND DATA ANALYSIS

The measurements in the gases were carried out following the sequence: N_2, H_2, D_2, N_2. A special run was also performed with the tube T evacuated to 10^{-3} torr.

In order to properly correlate the different runs the following procedure has been adopted:

1) we first searched the correct light incidence angle for the optical phase-shifter OPS by comparing the signals from the air Faraday cells FCA1 and FCA2, and following the method described in ref. [14]. The proper light incidence angle θ_i was found to be $\theta_i = 78.5^\circ \pm 0.25^\circ$.

2) Before starting any data-taking with the tube T filled of N_2, we adjusted the phases of the lock-ins. Therefore, once the gas was changed, the observed phase in the output birifringence signal of lock-in 2 was either 0° or 180° according on whether the gas under analysis had the C_{CM} constant of the same sign or opposite to that of N_2.

The runs for each gas were divided in subruns 500 seconds long to obtain a resolution of 2 mHz in the Fourier analysis in each subrun.

We recall that the intensity transmitted by crossed analyser and polariser prisms, to the lowest order in the ellipticity Ψ and in the polarization rotation Φ, is given by:

$$I = I_0 \, (\, \sigma^2 + \Psi^2 + \Phi^2 \,) \tag{6}$$

where I_0 is the light intensity prior to the analyser and σ^2 is the extinction factor of the system (in our case $I_0 \approx 10$ mW and $\sigma^2 \approx 10^{-7}$).

The ellipticity $\psi(t)$ induced by the rotating magnetic field is given by:

$$\psi(t) = \Psi_e \cdot [\sin(4\pi f_R t)] \cdot g(t) \tag{7}$$

where g(t) is the unit amplitude square-wave of period T = 100 seconds. For the case of N_2 the ellipticity peak-amplitude was $\Psi_e \approx 2.5 \cdot 10^{-7}$ in our experimental conditions.

In the cells FCA1,FCA2, and FCG the rotation of the polarization vector is given by:

$$\Phi_{a1}(t) = \Phi_A \cos(2\pi f_{a1} t + \phi_{a1}) \tag{8}$$

$$\Phi_{a2}(t) = \Phi_A \cos(2\pi f_{a2} t + \phi_{a2}) \tag{9}$$

$$\Phi_F(t) = \Phi_F \cos(2\pi f_F + \phi_F) \tag{10}$$

with $\Phi_A \approx 6 \cdot 10^{-7}$, $\Phi_F \approx 3 \cdot 10^{-4}$, and the initial phases taken into account. The quantities Ψ^2 and Φ^2 of expression (6), before the analyser, are given by:

$$\Psi^2(t) \approx 0 \tag{11}$$

$$\begin{aligned}\Phi^2(t) \approx \Phi_F \cos(2\pi f_F t + \phi_f) \cdot \{ & 2\Phi_A \cos(2\pi f_{a2} t + \phi_{a2}) \\ & + 2\rho_{\parallel}/\rho_{\perp}\, \Psi_e \sin(4\pi f_R t) \cdot [1/2 + 2/\pi \sin(2\pi f_{OF})] \\ & + \Phi_F \cos(2\pi f_F t + \phi_F) + 2\Phi_{mis}(t) + 2\rho_{\parallel}/\rho_{\perp}\, \Psi_{stray}(t)\}\end{aligned} \tag{12}$$

in which $\rho_{\parallel}$ and $\rho_{\perp}$ are the reflectivities of OPS for light linearly polarized parallel and orthogonal to the incidence plane respectively [14], $f_{OF} = 1/T = 10$ mHz is the on-off magnet current switching frequency, Ψ_{stray} is the small unavoidable ellipticity before OPS, and Φ_{mis} is the small misalignement between the analyser and the polarization vector.

We remark that, due to the synchronizing system, the phases of the signals at the frequency $2f_R$ and f_{OF} are zero with respect to the start of the data aquisition. In expression (12) we have retained only the two first terms of the Fourier series for g(t).

If we combine equations (6), (11), and (12) and remind that lock-in 1 is referred to the same signal driving the Faraday cell FCG, we derive the expression for the output signal:

$$V_1(t) = \eta I_0 R G_1/2 \{ 2\Phi_F\Phi_A \cos(2\pi f_{a2}t + \phi_{a2}) + 2\rho_{\parallel}/\rho_{\perp}\, \Phi_F\Psi_e \sin(4\pi f_R t)\cdot[1/2 + 2/\pi \sin(2\pi f_{OF}t)] + 2\Phi_F\cdot[\Phi_{mis}(t) + \rho_{\parallel}/\rho_{\perp}\, \Psi_{stray}(t)] \} + V_{noise}(t) \quad (13)$$

where $V_{noise}(t)$ is mainly due to the shot-noise in the photodetector current and to the laser intensity noise [3], G_1 is the amplification coefficient of lock-in 1; η is the photodiode efficiency ($\eta \approx 0.2$ A/W), and R is the feed-back resistor of the diode preamplifier (R = 400 MΩ).

The signal (13) is then processed by the lock-in 2 which is referred at the frequency $2f_R$. The output signal is given by:

$$V_2(t) = \eta I_0 R G_1 G_2/4\cdot\{ 2\Phi_F\Phi_A \cos[2\pi(f_{a2} - 2f_R)t + \phi_{a2}] + 2\rho_{\parallel}/\rho_{\perp}\, \Phi_F\Psi_e\cdot[1/2 + 2/\pi \sin(2\pi f_{OF}t)] \} + G_2 V_{noise}(t) + V_{pol}(t) \quad (14)$$

where G_2 is the amplification coefficient of lock-in 2 and $V_{pol}(t)$ is a noise signal due the Fourier component of $\Phi_{mis}(t)$ and $\Psi_{stray}(t)$ in the frequency region around $2f_R$.

From the on-line Fourier analysis of the signal (14) performed by the microcomputer at the end of each subrun we derive, for each gas, the quantity:

$$\Psi_e = \pi/2\cdot(\rho_{\parallel}/\rho_{\perp})\cdot(A_{gas}/A_{air})\cdot\Phi_A \quad (15)$$

where A_{air} is the Fourier amplitude of expression (14) at the frequency $f_{a2} - 2f_R$ = 24 mHz and A_{gas} is the projected Fourier amplitude at f_{OF} = 10 mHz.

Typical microcomputer amplitude spectra are presented in figs. 3 and 4 for H_2 and vacuum respectively. In this last case the Fourier amplitude at 10 mHz is at the noise level.

4. DATA ANALYSIS AND RESULTS

The Fourier amplitudes A_{gas} and A_{air} were first normalized to the standard conditions of gas pressure, magnetic field and FCA2 cell current excitation. To derive the Cotton-Mouton constant of H_2 and D_2 we have then analysed the distribution of the normalized ratios

$$R_{gas} = A_{gas}/A_{air} \tag{16}$$

of all subruns (see figs. 5 and 6) and we have then calculated the mean values $\langle R_{H_2} \rangle$, $\langle R_{D_2} \rangle$, and $\langle R_{N_2} \rangle$. The Cotton-Mouton constant of the gas relative to N_2 is given by:

$$C_{CM}(gas) = C_{CM}(N_2) \cdot \langle R_{gas} \rangle / \langle R_{N_2} \rangle \tag{17}$$

In formula (17) we will assume the following value for C_{CM} of N_2:

$$C_{CM}(N_2) = (-5.25 \pm 0.20) \cdot 10^{-17} \text{ Gauss}^{-2}\text{cm}^{-1} \tag{18}$$

at λ = 514.5 nm, 0°C, and 1 abs. atm., obtained by a weighted average of the values given in refs. [1,2]. The summary of the experimental data is

presented in table 3. From $\langle R_{N_2} \rangle$ and a direct measurement of the integral in formula (3) we found agreement within the experimental errors with value (18) for $C_{CM}(N_2)$.

The total error on the Cotton-Mouton constant $C_{CM}(gas)$ is derived taking into account the statistical error $\sigma_{gas}/\sqrt{N}$ on $\langle R_{gas} \rangle$, the error on $C_{CM}(N_2)$, and the extimated error ($\approx$2%) given by variations of the integral in formula (3). For H_2 and D_2 the statistical error $\sigma_{gas}/\sqrt{N}$ is dominant.

We remark that the spectrum of fig. 4 obtained in the run with vacuum in the tube T shows no significant signal component at the frequency f_{OF} = 10 mHz but a peak at 0 Hz, probably due to residual mechanical vibrations; this justifies the use of the double modulation tecnique.

Our experimental results for H_2 and D_2 are compared in table 4 with the values obtained from formula (2) using the theoretical and experimental data of tables 1 and 2. The agreement is very good within the experimental errors.

From formula (2) and from the values of $C_{CM}(H_2)$ and $C_{CM}(D_2)$ that we have measured, we obtain:

$$(\Delta\beta \cdot \Delta\chi)|_{H_2} = (1.68 \pm 0.17) \text{ erg cm}^3 \text{ mole}^{-1} \quad (19)$$

$$(\Delta\beta \cdot \Delta\chi)|_{D_2} = (1.48 \pm 0.19) \text{ erg cm}^3 \text{ mole}^{-1} \quad (20)$$

at λ = 514.5 nm and 0°C. The uncertitude on formula (2) due to the theoretical approximations is not taken into account in expressions (19) and (20). These expressions determine the allowed regions for $\Delta\chi$ versus $\Delta\beta$;

they overlap the regions given by the values of tables 1 and 2 as shown in figs. 7 and 8. The overall agreement is very good.

ACKNOWLEDGMENTS

We thank the technical group of W. Albrecht (EP division, CERN) for making the design of the rotating magnet support, and R. Grabit, F. Jeanmairet, M. Moretti and B. Smith for their technical help. We are grateful to P. Bernard for the use of the laboratory facilities.

References

[1] A.D. Buckingham, W.H. Prichard, and D.H. Whiffen, Trans. Faraday Soc., 63, 1057 (1967)

[2] S. Carusotto, E. Polacco, E. Iacopini, G. Stefanini, and E. Zavattini, Opt. Comm., 42, 104 (1982)

[3] S. Carusotto, E. Iacopini, E. Polacco, F. Scuri, G. Stefanini, and E. Zavattini, J. Opt. Soc. Am., 1B, 635 (1984)

[4] A.D. Buckingham and J.A. Pople, Proc. Phys. Soc.(London), 69B, 1133 (1956)

[5] S. Kielich, Acta Phys. Polonica, 22, 299 (1962)

[6] T. Neugebauer, Zeitschrifts fur Physik, 112, 257 (1939)

[7] J. Rychlewski, J. Chem. Phys., 78, 7252 (1983)

[8] F. Bass and K.D. Van der Hout, Physica, 95A, 597 (1979)

[9] J. Rychlewski and W.J. Raynes, Mol. Phys., 41, 843 (1980)

[10] W.H. Flygare and R.C. Benson, Mol. Phys., 20, 225 (1971)

[11] G.W. Parker and J.D. Memory, Phys. Rev., 23A, 2099 (1981)

[12] R.G. Barnes, P.J. Bray, and N.F. Ramsey, Phys. Rev., 94, 893 (1954)

[13] A.D. Buckingham and J.E. Cordle, Mol. Phys., 28, 1037 (1974)

[14] S. Carusotto, E. Iacopini, E. Polacco, F. Scuri, G. Stefanini, and E. Zavattini, Appl. Phys., 36B, 125 (1985)

Table 1

Electrical polarizability anisotropies in H_2 and D_2; $\Delta\beta = \beta_{\parallel} - \beta_{\perp}$

Gas	λ nm	$\Delta\beta_{th} \times 10^{25}$ cm^3	$\Delta\beta_{exp} \times 10^{25}$ cm^3	ref.
H_2	546.2	3.15		7
"	436.0	3.21		7
"	514.5		3.0±0.1	10
D_2	546.2	3.06		7
"	436.0	3.11		7
"	514.5		2.9±0.1	10

Table 2

Magnetic susceptibility anisotropies for H_2 and D_2 in the visible region. $\Delta\chi = \chi_{\parallel} - \chi_{\perp}$; $\Delta\chi$ is given in erg×Gauss^{-2}×mole^{-1}

gas	$\Delta\chi_{th}\times10^6$	$\Delta\chi_{exp}\times10^6$	ref.
H_2	0.605		8
"	0.535		9
"		0.553±0.02	11
"		0.551±0.03	12
"		0.536±0.02	13
D_2	0.523		9
"		0.527±0.06	12
"		0.524±0.02	13

Table 3

Summary of the experimental data for the C_{CM} constant for H_2, D_2 and N_2. C_{CM} is given in $Gauss^{-2} \times cm^{-1}$ at λ = 514.5 nm, 0°C and 1 abs. atm.

Gas	subruns	$\langle R_{gas} \rangle$	σ_{gas}	$\sigma_{gas}/\sqrt{N}$	$C_{CM} \times 10^{18}$
H_2	47	.0116	.0036	.0005	1.61±0.11
D_2	30	.0103	.0046	.0008	1.41±0.14
N_2	5	.3793	.0015	.0007	-52.5±2.0[a]

a) Refs. [1,2]

Table 4

C_{CM} constants of H_2 and D_2 at λ = 514.5 nm, 0°C, and 1 abs.atm.

Gas	$\Delta\beta\times10^{25}$ cm^3	$\Delta\chi\times10^{6}$ erg $G^{-2}mole^{-1}$	$C_{CM}\times10^{18}$ $G^{-2}cm^{-1}$
H_2	3.0±0.1 [a]	.544±.02 [c]	1.56±0.12 [d]
"	3.18 [b]	.570 [b]	1.73
"	-	-	1.61±0.11 [e]
"	-	-	1.80±2.30 [f]
D_2	2.9±0.1 [a]	.525±.02 [c]	1.45±0.11 [d]
"	3.08 [b]	.523 [b]	1.53
"	-	-	1.41±0.14 [e]

a) λ= 514.5 nm, ref. [10] (experimental).

b) average of the calculated values given in refs. [7-9]

c) average of the measured values given in refs. [11-13]

d) phenomenological value obtained using formula (2); the error accounts the experimental errors on the quantities $\Delta\beta$ and $\Delta\chi$.

e) value obtained in this experiment with the total error.

f) Value given by Buckingham et al. [1]; their measurements were done in compressed gases and at 20°C but the C_{CM} value is reported at normal conditions of temperature and pressure.

FIGURE CAPTIONS

Fig.1 : Experimental apparatus: optical layout.
A: analyser prism; BS: beam splitter; C: compensator;
D1, D2: photodiodes; FCA1, FCA2: air Faraday cells;
FCG: glass Faraday cell; HWP: half-wave plate; L1, L2: lenses;
M1, M2: mirrors; OPS: optical phase-shifter; P: polarizer prism;
PC: pick-up coil; SC: synchronizing coil; STM: stepping motor;
T: gases tube; TL: telescope; W1, W2: windows.

Fig.2 : Experimental apparatus: electronics layout.

Fig.3 : Fourier amplitude spectrum of the lock-in 2 output for H_2.
The peak at f_{OF} = 10 mHz corresponds to the birefringence signal and the peak at $f_{a2} - f_R$ = 24 mHz corresponds to the reference signal produced by the FCA2 Faraday air cell.
The integration time is 500 seconds.

Fig.4 : Fourier amplitude spectrum of the lock-in 2 output for vacuum.
The integration time is 8000 seconds.

Fig.5 : Histogram of the distribution of the R_{gas} ratios for D_2.
The dashed curve is the Gaussian with mean value $\langle R_{D_2} \rangle$ and r.m.s. deviation σ_{D_2}.

Fig.6 : Histogram of the distribution of the ratios R_{gas} for H_2.
The dashed curve is the Gaussian with mean value $\langle R_{H_2} \rangle$ and r.m.s. deviation σ_{H_2}.

Fig.7 : Allowed regions for $\Delta\beta$ and $\Delta\chi$ from the previous experimental data in H_2 [10-13] (thin lines) and for $(\Delta\beta \cdot \Delta\chi)$ from our results (thick lines). The dashed lines represent the averages of the theoretical data [7-9].

Fig.8 : Allowed regions for $\Delta\beta$ and $\Delta\chi$ from the previous experimental data in D_2 [10,12,13] (thin lines) and for $(\Delta\beta \cdot \Delta\chi)$ from our results (thick lines). The dashed lines represent the averages of the theoretical data [7,9].

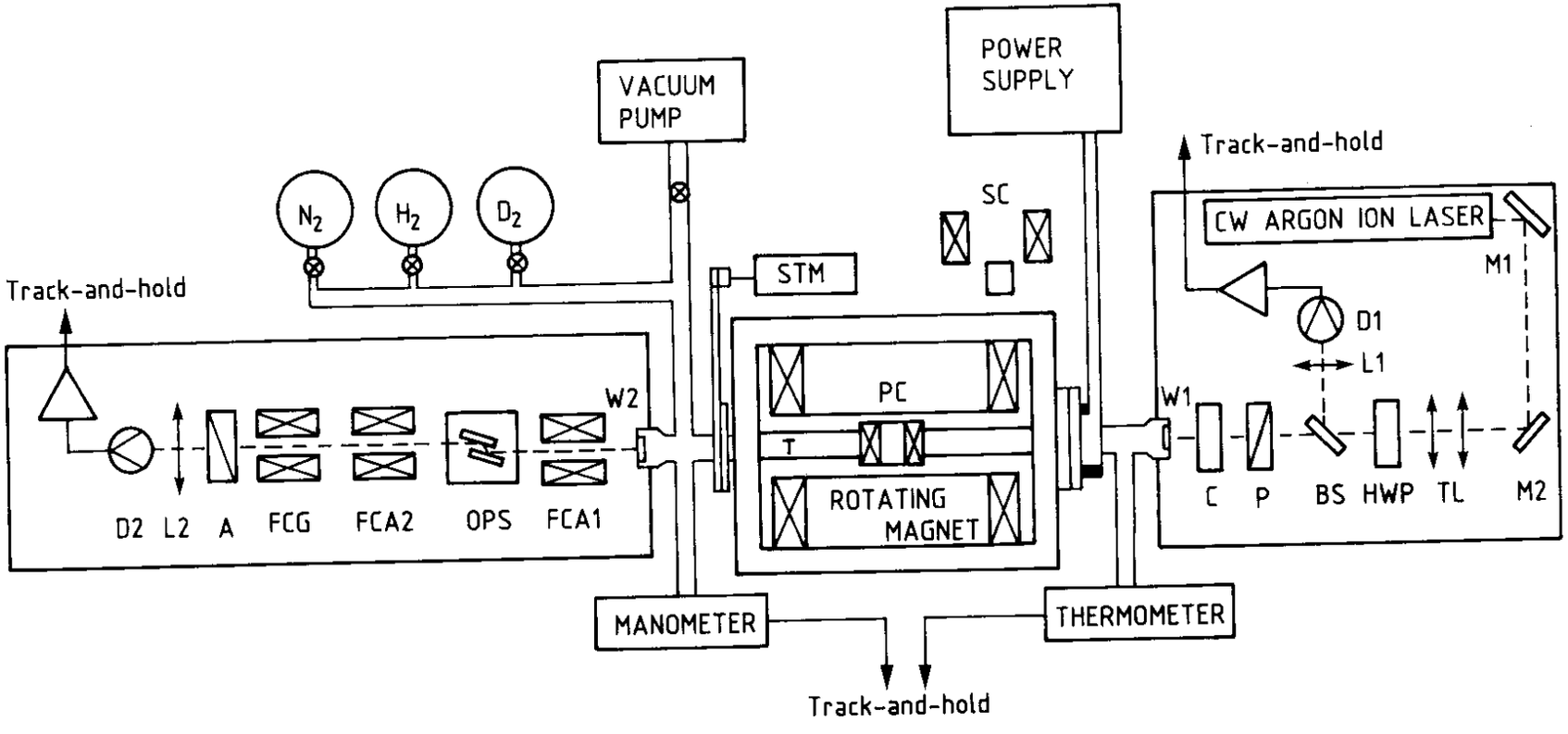
VACUUM PUMP
POWER SUPPLY
Track-and-hold
N_2
H_2
D_2
SC
STM
CW ARGON ION LASER
M1
Track-and-hold
D1
L1
PC
W2
W1
T
ROTATING MAGNET
D2 L2 A FCG FCA2 OPS FCA1
C P BS HWP TL M2
MANOMETER
THERMOMETER
Track-and-hold

Fig. 1

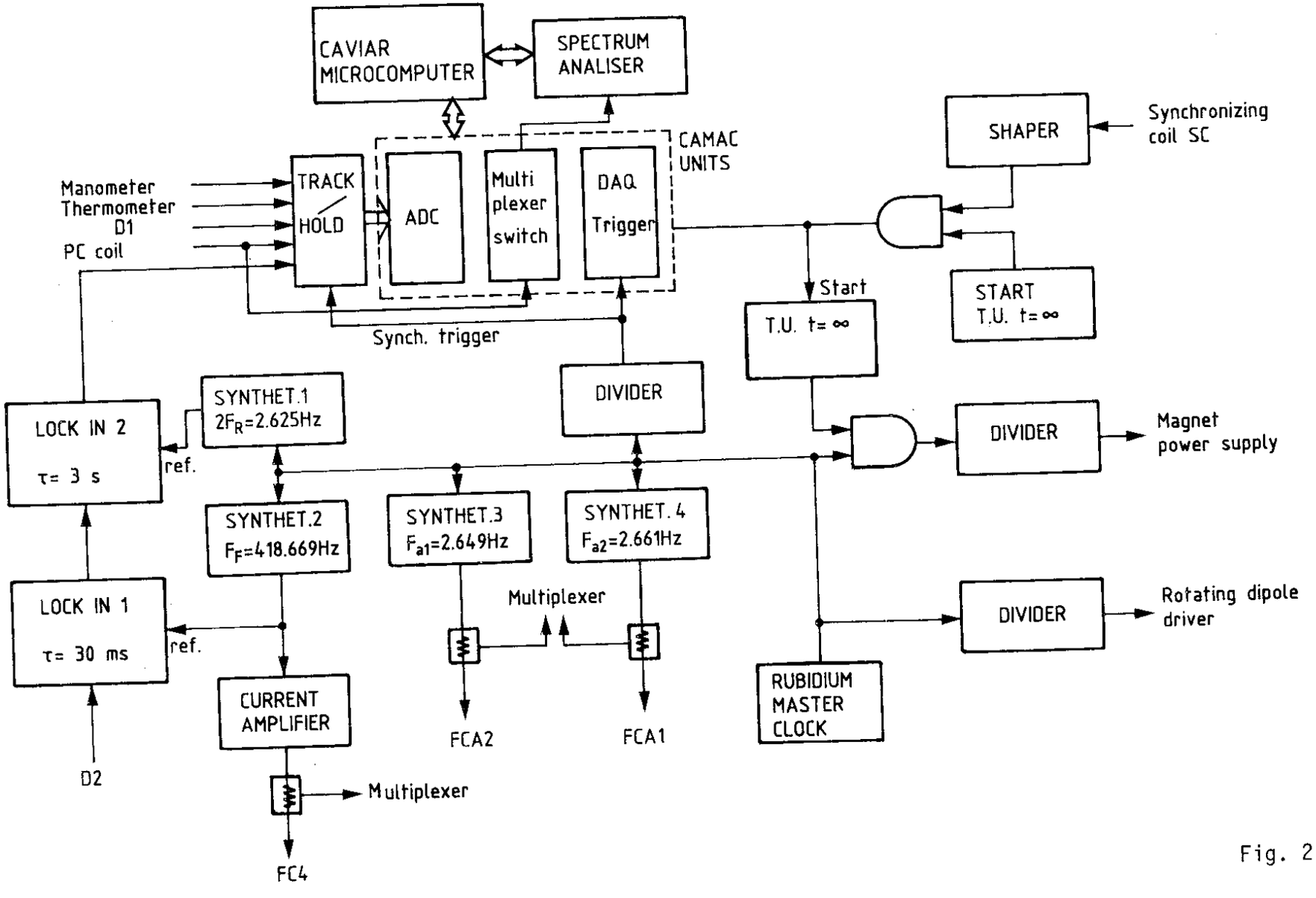
CAVIAR MICROCOMPUTER
SPECTRUM ANALISER
CAMAC UNITS
TRACK HOLD
ADC
Multi plexer switch
DAQ Trigger
Manometer
Thermometer
D1
PC coil
Synch. trigger
SHAPER
Synchronizing coil SC
START T.U. t= ∞
Start
T.U. t= ∞
DIVIDER
DIVIDER
Magnet power supply
LOCK IN 2
τ= 3 s
ref.
SYNTHET.1
2F_R=2.625Hz
SYNTHET.2
F_F=418.669Hz
SYNTHET.3
F_a1=2.649Hz
SYNTHET. 4
F_a2=2.661Hz
Multiplexer
LOCK IN 1
τ= 30 ms
ref.
CURRENT AMPLIFIER
FCA2
FCA1
RUBIDIUM MASTER CLOCK
DIVIDER
Rotating dipole driver
D2
Multiplexer
FC4

Fig. 2

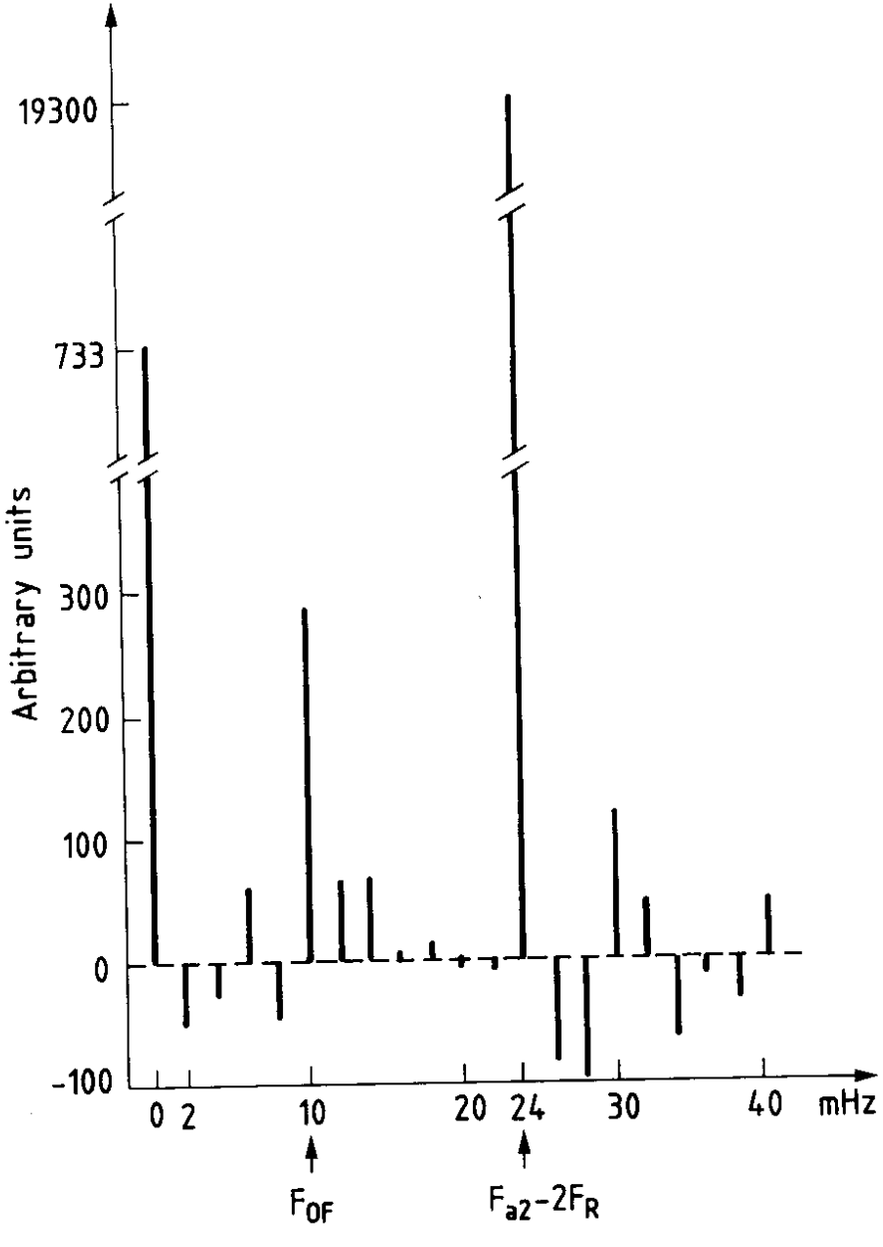
19300
733
Arbitrary units
300
200
100
0
-100
0 2
10
20 24
30
40 mHz
F_{OF}
$F_{a2}-2F_R$

Fig. 3

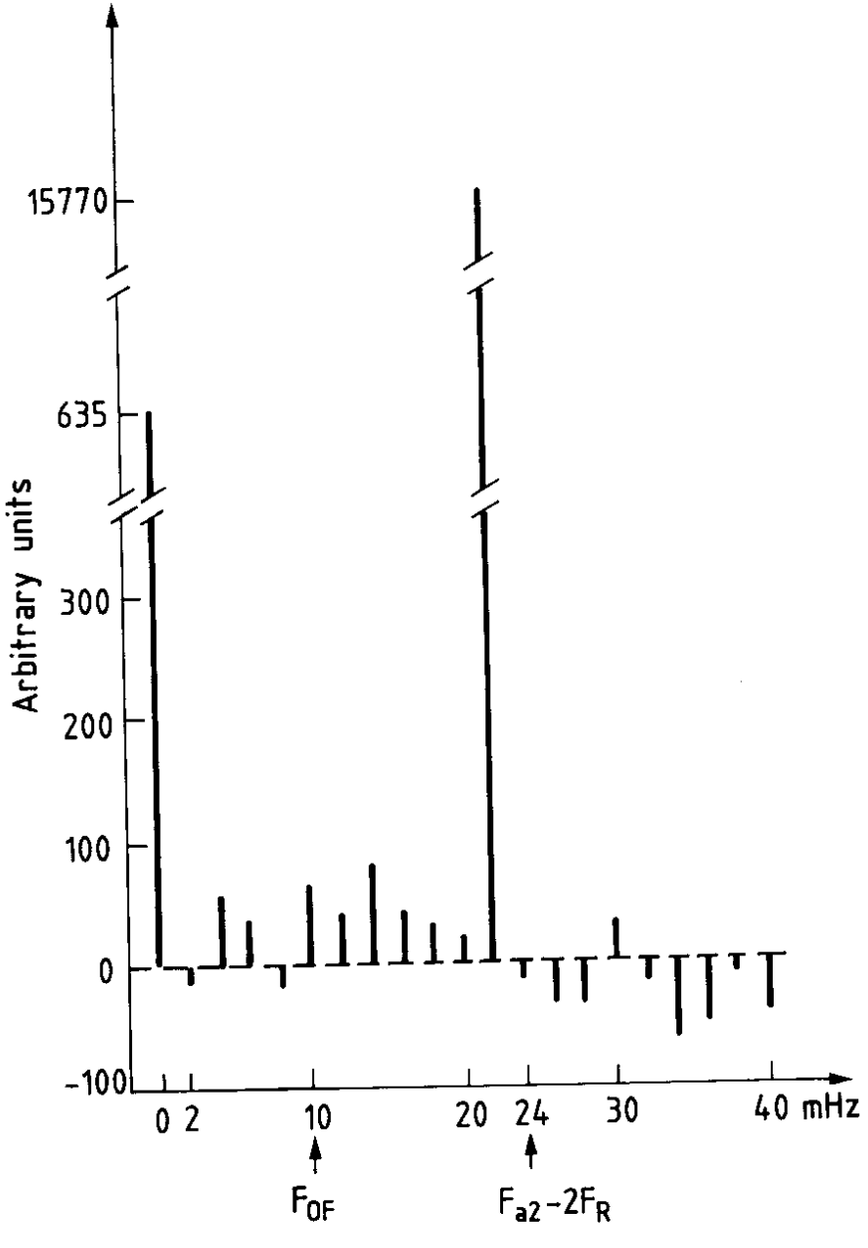
15770
635
Arbitrary units
300
200
100
0
-100
0 2
10
20 24
30
40 mHz
F_{OF}
$F_{a2}-2F_R$

Fig. 4

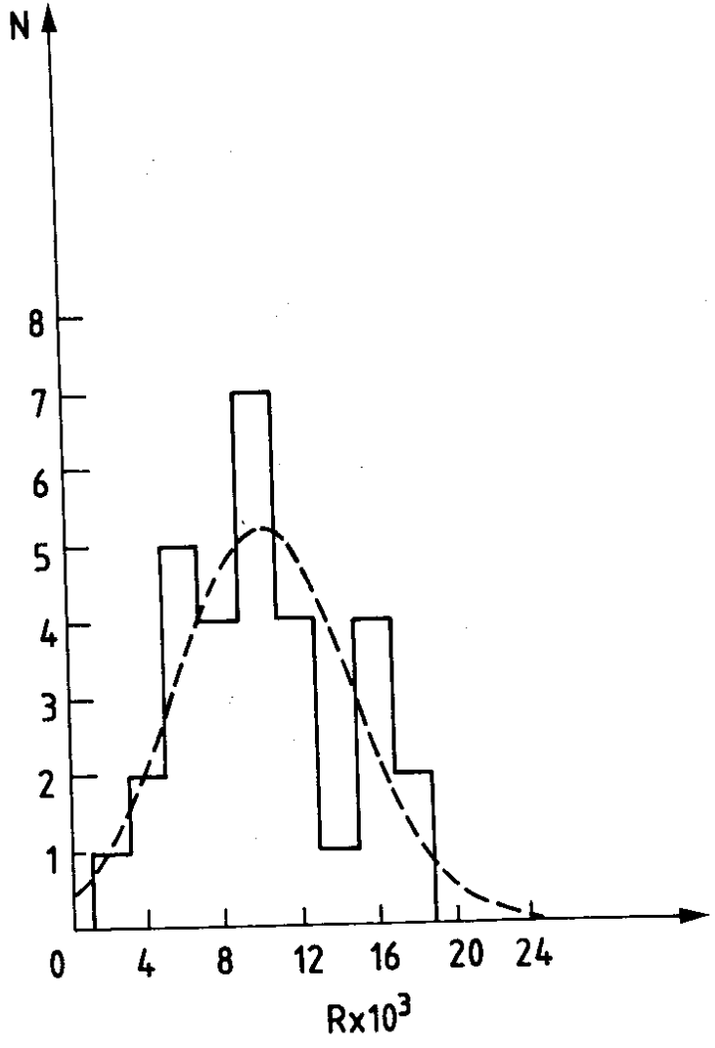
N
8
7
6
5
4
3
2
1
0
4
8
12
16
20
24
Rx10³

Fig. 5

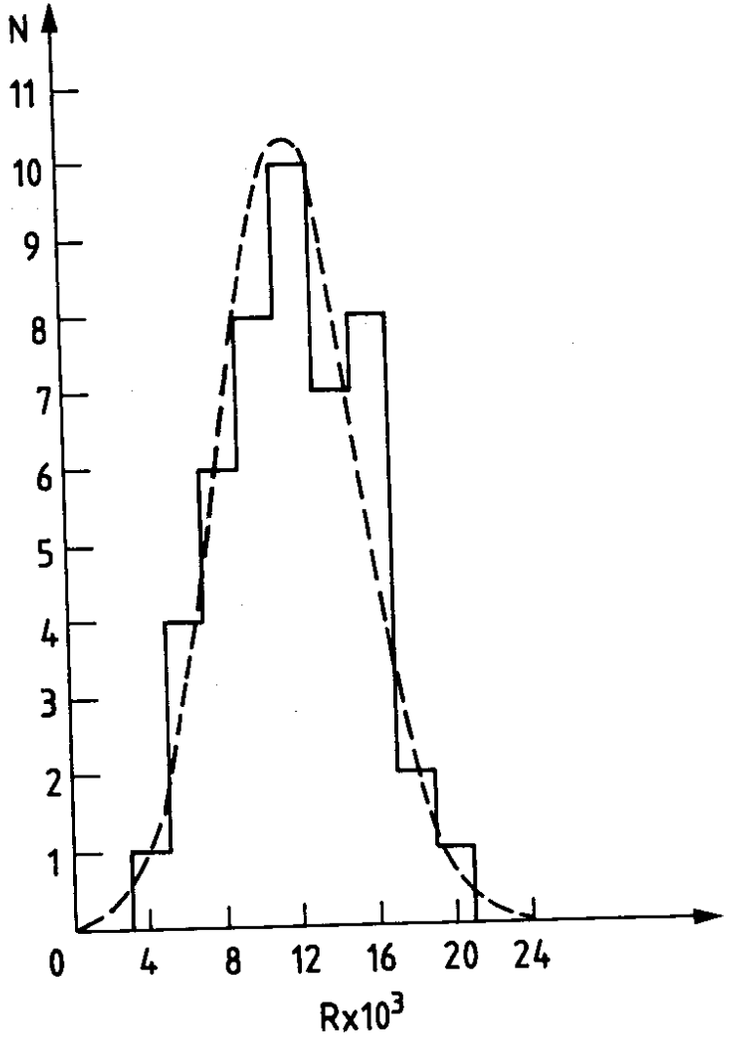
N
11
10
9
8
7
6
5
4
3
2
1
0
4
8
12
16
20
24
Rx10³

Fig. 6

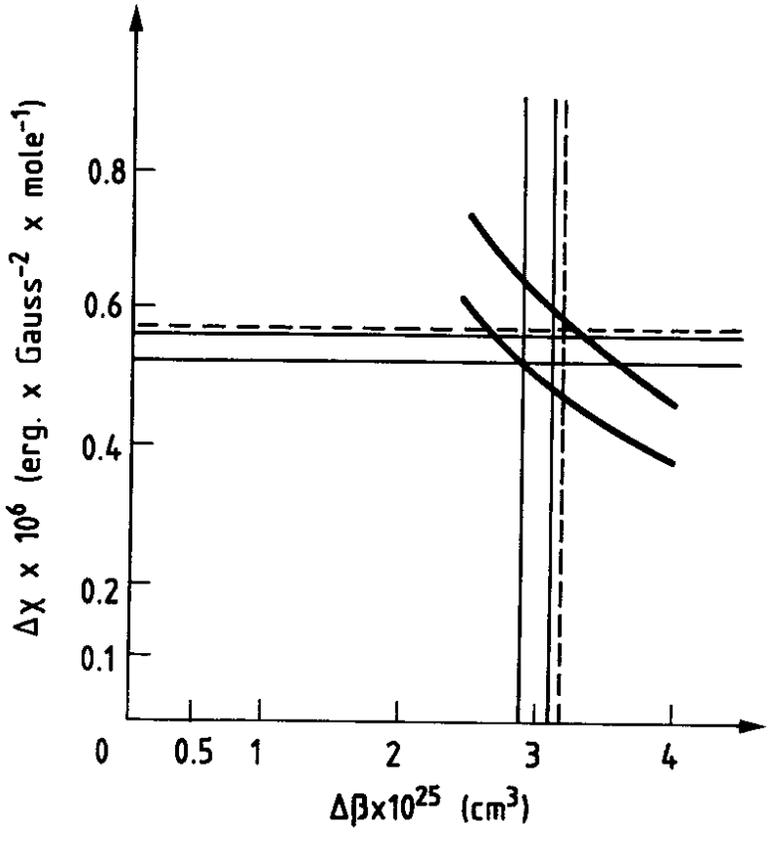
$\Delta\chi \times 10^6$ (erg. x Gauss^{-2} x mole^{-1})
0.8
0.6
0.4
0.2
0.1
0
0.5
1
2
3
4
$\Delta\beta \times 10^{25}$ (cm^3)

Fig. 7

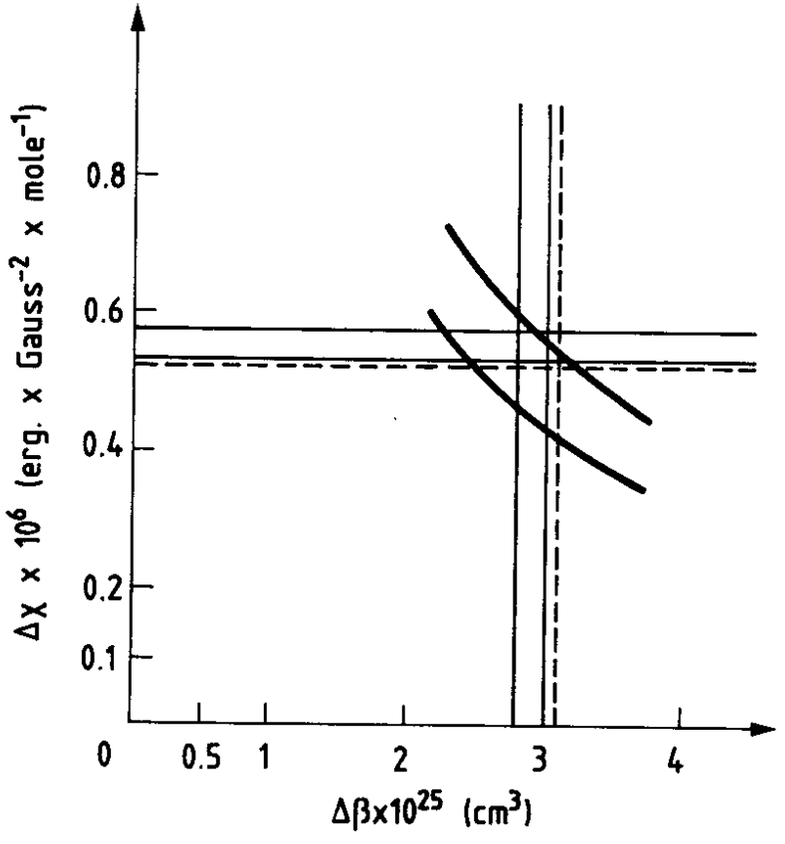
$\Delta\chi \times 10^6$ (erg. x Gauss^{-2} x mole^{-1})
0.8
0.6
0.4
0.2
0.1
0
0.5
1
2
3
4
$\Delta\beta \times 10^{25}$ (cm^3)

Fig. 8